COUPLING OF NUMERICAL MAGNETIC AND EXPERIMENTAL VIBRATION ANALYSIS FOR ELECTRICAL MACHINES

Koen Delaere, Michele Iadevaia†, Paul Sas†, Ronnie Belmans and Kay Hameyer
Dept. EE (ESAT), Div. ELEN †Dept. Mechanics, Div. PMA
Katholieke Universiteit Leuven, B3000 Leuven, Belgium
E-mail: Koen.Delaere@esat.kuleuven.ac.be, http://www.esat.kuleuven.ac.be/elen/elen.html

Abstract – The vibration spectrum of the stator of a 6-pole synchronous machine is analysed. First, a fully numerical vibration analysis is performed, using magnetical and mechanical 2D finite element models. This analysis makes use of modal participation factors, i.e. the correlation between instantaneous force patterns inside the machine and the stator mode shapes. Second, the stator's vibration spectrum during no-load generator operation is determined experimentally. Third, the stator mode shapes are determined using experimental modal analysis. The results from the experimental and numerical vibration analysis are compared and related to the experimental modal analysis of the stator.

Keywords: finite element methods, electromagnetic forces, modal analysis, vibration control, coupled problems.

1. Introduction

Stator vibrations are the main source of acoustic noise of electric machines. The stator vibrations are determined by the stator mode shapes and the excitation due to the magnetic field in the air gap. The mode shapes of the stator can be calculated using 2D or 3D mechanical finite element (FE) models, or they can be measured experimentally. The magnetic field exerts radial forces on the stator teeth, due to Maxwell's magnetic stress at the interface between media of different permeability. To take stator deformations into account, a local magnetic force formulation is needed. An FE based expression for local electromagnetic forces is derived using the virtual work principle. The *mode participation factor* (generalised modal force) is used to express the correlation between all significant stator modes and a specific force distribution. Subsequently, these mode participation factors (MPF) are calculated for all relevant rotor positions, corresponding to different time instants. The frequency spectrum of the MPF and the mechanical impedance of the individual mode shapes lead to an estimate of the stator's vibration spectrum. This analysis can be performed using mode shapes obtained numerically, or using mode shapes determined experimentally. The vibration spectrum obtained is compared to the vibration spectrum measured.

2. Local electromagnetic forces

Both magnetostatic and elasticity FE methods are based upon the minimisation of an energy function. The total energy E of the electromechanical system consists of the *elastic energy* U stored in a body with deformation a[1] and the *magnetic energy* W stored in a linear magnetic system with vector potential A[2]:

$$E = U + W = \frac{1}{2} a^T K a + \frac{1}{2} A^T M A \tag{1}$$

where K is the mechanical stiffness matrix and M is the magnetic 'stiffness' matrix. Considering the similar form of these energy terms, the following system of equations represents the numerically coupled magneto-mechanical system:

$$\begin{bmatrix} M & D \\ C & K \end{bmatrix} \begin{bmatrix} A \\ a \end{bmatrix} = \begin{bmatrix} T \\ R \end{bmatrix} \tag{2}$$

where T is the magnetical source term vector. R represents forces other than those of electromagnetic origin. Setting the partial derivatives of total energy E with respect to the unknowns $[A \;\; a]^T$ to zero, the combined system (2) with T=0, R=0 is retrieved:

$$\frac{\partial E}{\partial A} = M A + \frac{1}{2} a^T \frac{\partial K(A)}{\partial A} a = 0 , \tag{3}$$

$$\frac{\partial E}{\partial a} = K a + \frac{1}{2} A^T \frac{\partial M(a)}{\partial a} A = 0 . \tag{4}$$

The coupling term C can thus be recognised as

$$C = \frac{1}{2} A^T \frac{\partial M(a)}{\partial a} . \tag{5}$$

This coupling term represents the dependency of magnetic parameters on the mechanical displacement, e.g. permeability changes due to density or stress variations, but also magnetic energy variation due to geometry changes. Using (5) and neglecting external forces (R=0), the second equation in (2) is rearranged into

$$K a = -\frac{1}{2} A^T \frac{\partial M(a)}{\partial a} A = F_{em} . \tag{6}$$

Table 1 Main properties of 6-pole SM machine

rotor outer radius	73.5 mm
stator inner radius	75.0 mm
rotor field excitation	5 A
emf	127 Vrms
maximum flux density	1.0 T

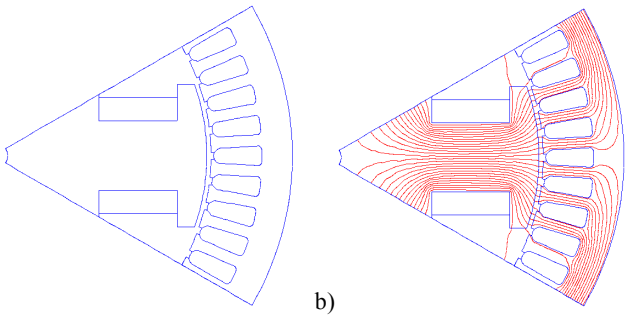

a) b)

Fig. 1 a) Geometry of one pole of the 6-pole SM, b) Magnetic field for rotor position 0º.

This reveals a means to calculate the nodal electromagnetic reluctance forces F_{em} from vector potential A and the *partial derivative* of the magnetic stiffness matrix M with respect to deformation a. The validity of (6) has been tested against analytical models. The forces F_{em} can also be found by applying the virtual work principle to the magnetic energy W considering a virtual displacement a[3-4]:

$$F_{em} = -\frac{\partial W}{\partial a} = -\frac{\partial}{\partial a}\left[\frac{1}{2} A^T M A\right]. \qquad (7)$$

The vector potential A has to remain unchanged as the nodes move through their virtual displacement ∂a[5]. Since ∂a alters the element area, the level of saturation changes and yields a different value for permeability μ. In a saturated system, (7) can still be used if the permeability dependence of M is taken into account in the partial derivative. However, a reasonable approximation can be made by fixing the element's permeability to the value found after solving the non-linear magnetic problem.

3. Numerical magneto-mechanical analysis

3.1 Mode participation factors

The main properties of the synchronous machine (SM) are given in Table 1. The geometry of one pole of the 6-pole SM is shown in Fig.1a. When the rotor coil is current excited, it generates the magnetic field shown in Fig.1b. This magnetic field is used to evaluate the local reluctance forces F_{em} on the stator, shown in Fig.2 for rotor position 0º. These forces are pointing inwards and do not add to the torque; they only cause stator deformation.

Using the 2D mechanical stiffness matrix K and mass matrix M_m, the undamped 2D stator mode shapes are found, some of which are shown in Fig.3. The modes are calculated taking into account the stator iron, the stator coil copper (both mass and stiffness) and the rigid machine mounting. For a given rotor position, the mode participation factors Γ_i are found by correlating the actual force pattern f with the mode shapes ϕ_i (and not with the actual deformation a)[6]:

$$\Gamma_i = \frac{\phi_i^T f}{\phi_i^T M_m \phi_i} \qquad (8)$$

where ϕ_i is the i^{th} mode shape and f is the force distribution for this rotor position. The j^{th} element of the vector ϕ_i is the displacement of the i^{th} mode shape at the j^{th} node. Similarly, $f(j)$ is the force at the j^{th} node.

Table 2 lists the eigenfrequencies and the MPF of the first 18 modes for rotor position 0º. Fig.4 shows the MPF of modes 8, 14, 15, 17 for all rotor positions, calculated in 2º steps. The MPF of all other modes stays below 2, except modes 5 and 12. Due to the machine symmetry, all MPF behave periodically over 60º rotor

Table 2 Mode participation factors for rotor position 0º

mode number	freq. (Hz)	MPF	mode number	freq. (Hz)	MPF
1	55	–0.0123	*10*	655	–1.7921
2	123	**2.4439**	*11*	704	0.5842
3	264	–0.3395	*12*	752	**8.7069**
4	271	–0.4586	*13*	885	–1.7793
5	379	**18.7630**	*14*	954	**3.1976**
6	413	1.3822	*15*	1249	**6.1018**
7	442	**7.5528**	*16*	1084	–1.9335
8	525	–1.0014	*17*	1111	**2.5362**
9	573	0.0703	*18*	1276	**–2.9673**

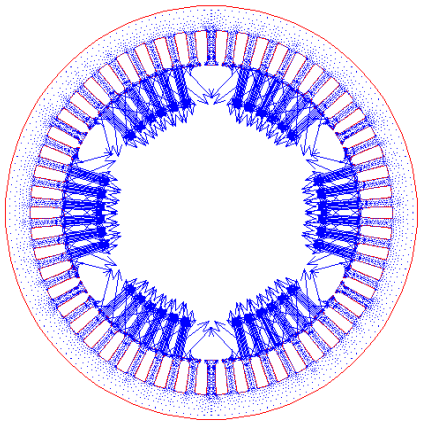

Fig. 2 Force distribution F_{em} acting on stator for rotor position 0º.

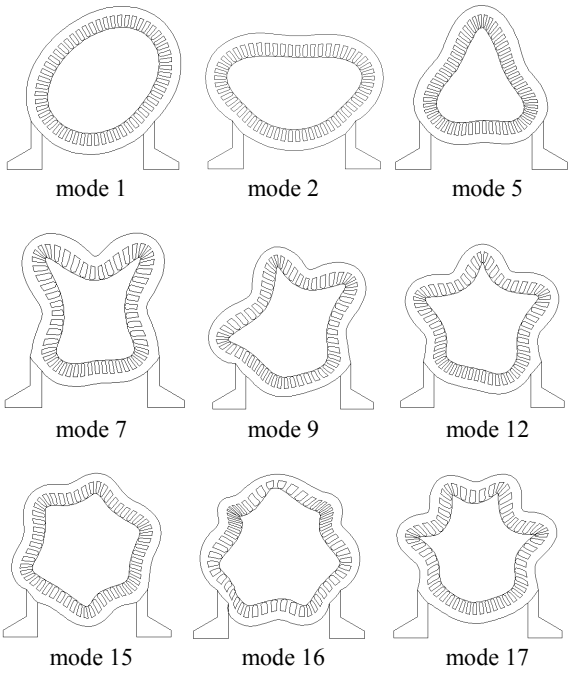

Fig. 3 Selected mode shapes for the 6-pole SM stator structure with rigid mounting.

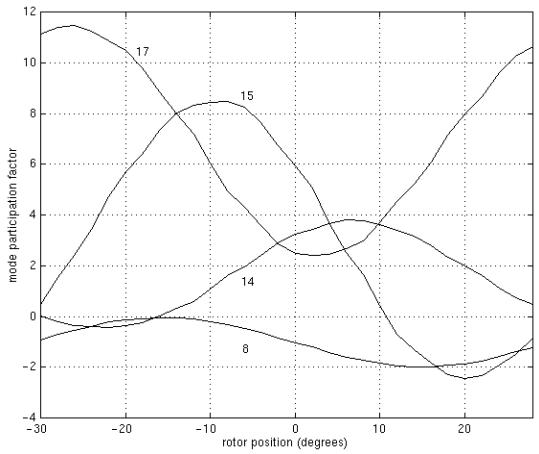

Fig. 4 Mode participation factor as a function of rotor position.

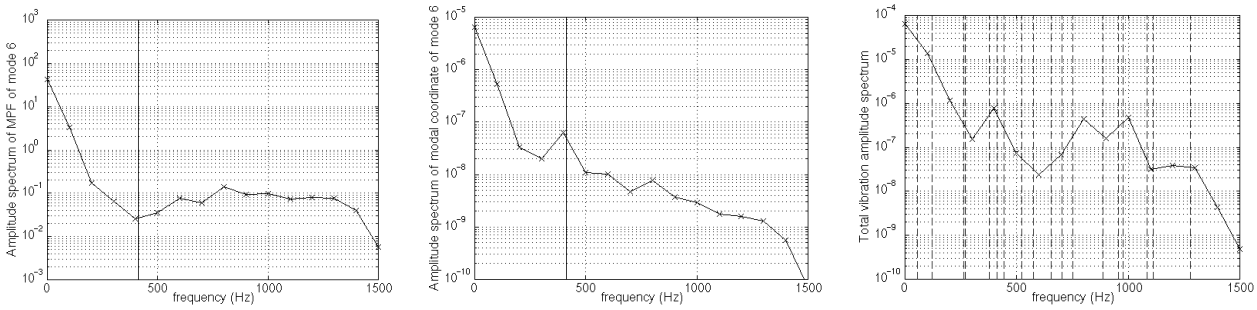

Fig. 5 a) Discrete amplitude spectrum $\Gamma_6(k\Delta f)$ of the MPF of the 6th mode (eigenfrequency 413 Hz).
b) Discrete amplitude spectrum $Q_6(k\Delta f)$ of the generalised co-ordinate $q_6(t)$ of mode 6.
c) Total vibration spectrum as a sum of modal spectra.

displacement. The MPF usually contain both a DC- and an AC-component. Modes 5, 7 and 2 have an almost constant MPF of approximately 19, 7 and 3 respectively; these correspond with constant (generalised) forces wanting to 'collapse' the stator. This leads to some shrinking of the stator, but no vibrations are produced.

3.2 Modal decomposition

The vibration of the stator is governed by

$$M_m\ddot{a} + C_m\dot{a} + Ka = f(t)\,, \tag{9}$$

where $a(t)$ is the nodal displacement and $f(t)$ is the force pattern acting on the stator. Using the modal decomposition

$$a = Pq\,, \tag{10}$$

with P the modal matrix containing a selected set of N stator mode shapes and q the vector of generalised modal co-ordinates, (9) is transformed into

$$P^T M_m P\ddot{q} + P^T C_m P\dot{q} + P^T KPq = P^T f(t)\,, \tag{11}$$

where all terms were premultiplied by P^T. Only when the mechanical damping C_m is assumed to be proportional ($C_m = \alpha K + \beta M_m$), the system of equations (11) can be decoupled into[7]

$$\ddot{q}_i + 2\zeta_i\omega_i\dot{q}_i + \omega_i^2 q_i = \Gamma_i(t)\,,\ i = 1..N. \tag{12}$$

where ω_i is the mode eigenfrequency and ζ_i is the modal damping factor. Here damping is neglected ($\zeta_i=0$) and only the 18 modes of Table 2 are considered. Note that the modal decomposition indeed transforms the force $f(t)$ into the MPF $\Gamma_i(t)$, $i = 1..18$, as prescribed by (8). Since the MPF are known as a function of rotor position, the rotor speed allows us to find the MPF as a function of time. The separate equations (12) are solved in the frequency domain after applying a discrete Fourier transformation on $q_i(t)$ and $\Gamma_i(t)$:

$$Q_i(k\Delta\omega) = \frac{\Gamma_i(k\Delta\omega)}{\omega_i^2 - (k\Delta\omega)^2}\,. \tag{13}$$

Fig.5a shows, in semi-log scale, the discrete amplitude spectrum $\Gamma_6(k\Delta f)$ of the MPF of the 6th mode with eigenfrequency f_6=413 Hz (indicated by the vertical line). Fig.5b shows the corresponding amplitude spectrum $Q_6(k\Delta f)$ of the generalised co-ordinate $q_6(t)$ calculated using (13). The higher frequency components are attenuated more than the lower frequency components, due to the relatively low value of f_6. Around f_6, there is a local amplification of the response of this mode.

3.3 Total vibration spectrum

The spectrum of any individual mode shape can be found as described above. The separate complex spectra of the relevant modes are summed to give the machine's total vibration spectrum. Fig.5c shows the amplitude spectrum of the sum of the spectra of the 18 selected modes. The eigenfrequencies of the 18 modes are indicated by the vertical lines. This total spectrum represents the stator vibration as predicted by the numerical 2D magnetical and mechanical model.

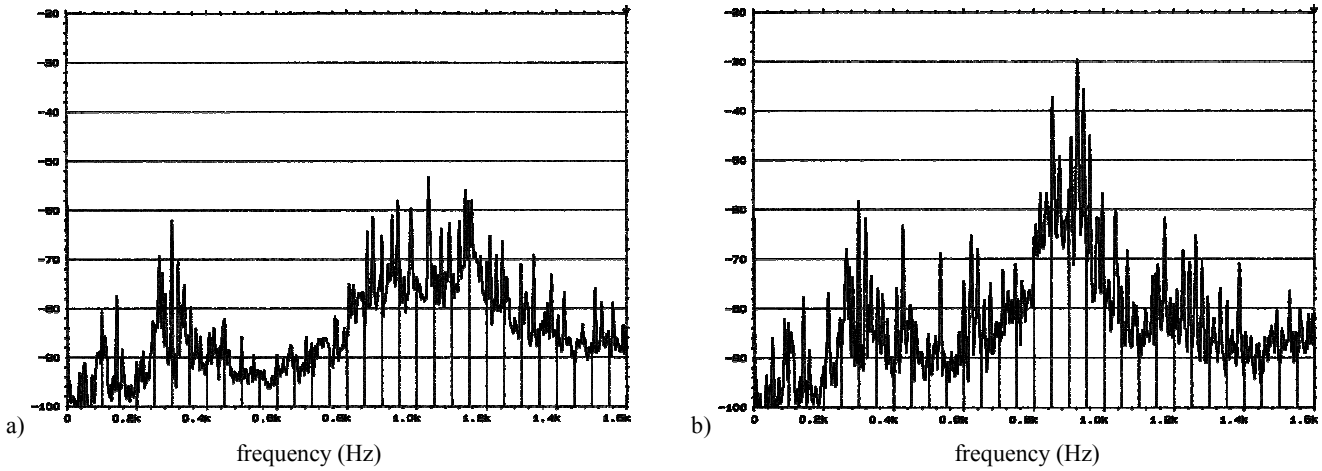

Fig. 6 Experimentally determined vibration spectrum of SM stator surface a) without rotor excitation and b) with rotor excitation.

Table 3 Eigenfrequencies of stator structure without coils

mode number	freq. (Hz)	mode number	freq. (Hz)
1	472.9	*8*	1041.3
2	608.3	*9*	1184.3
3	694.5	*10*	1199.9
4	725.6	*11*	1224.1
5	729.2	*12*	1232.8
6	780.2	*13*	1423.5
7	785.5	*14*	1504.2

3.4. Experimental verification

The synchronous machine is measured during no-load generator operation, driven at 1000 rpm by a DC motor. By applying a single accelerometer to the stator surface, two vibration spectra are measured: one before and one after applying the rotor excitation. The spectrum in Fig.6a represents stator vibrations of mechanical origin only (or introduced by the motor control of the driving DC machine), since no electric or magnetic field is present in the machine during this measurement. Fig.6b shows the vibrations caused by both the mechanical system and the magnetic field in the air gap (rotor excitation $I_b = 7$ A). The magnetic field introduces additional peaks in almost the whole frequency band measured.

The difference between the spectra in Fig.6a and Fig.6b has to be compared with the spectrum in Fig.5c. The numerical 2D models predict that vibrations induced by the magnetic field occurs mainly around 400 Hz and in the frequency band 750 Hz – 1100 Hz. Fig.6 confirms that these frequency bands are indeed sensitive to a large increase of vibrational components caused by the magnetic field. The pure DC-component in Fig.5c represents the static deformation of the stator discussed earlier and cannot be verified using an accelerometer.

The prediction in Fig.5c fails at the low frequency side. The fundamental force components at 100 Hz and 200 Hz occurring in the models are not found with the same magnitude in the experiment. The numerical 2D model overestimates the importance of these fundamental components. Further research will indicate whether this difference can be resolved using 3D mechanical finite element models, with or without modelling the stator coil damping.

4. Experimental modal analysis

An experimental modal analysis (EMA) is performed on the stator of an identical synchronous machine, in order to find the most important mode shapes and their eigenfrequencies[8]. The rotor, the end caps and the total electrical system (contacts, stator coils, etc.) are removed from the machine. Table 3 lists the eigenfrequencies of the first 14 modes.

Comparing Table 2 and Table 3, it is seen that the 2D mechanical model underestimates the model density of the stator[9]; the calculated 2D modes are spaced more evenly than the measured modes. Also, the 2D model predicts more modes in the region below 470 Hz, while the EMA does not detect stator modes in this region.

The influence of the stator coils (mass and damping) and the presence of the end caps on the stator mode shapes has to be estimated by repeating the EMA for a stator with stator coils (and end caps).

5. Conclusion

A finite element based expression for local electromagnetic reluctance forces is presented. The stator's modal shapes are calculated using a 2D mechanical finite element model. The mode shapes are correlated with the force distributions for all relevant rotor positions. From the resulting mode participation factors, the vibration spectrum of the individual modes is found. Summing these complex mode spectra gives the total vibration frequency spectrum of the machine, which in this way can be anticipated at the design level. The numerical prediction of vibrations caused by the magnetic field corresponds well with the difference between the measured vibration spectra before and after rotor excitation. This technique of vibration prediction using mode participation factors is very promising, considering the fact that even the use of simple 2D models yields good results. Future research will focus on more accurate modelling in 3D.

Acknowledgement

The authors are grateful to the Belgian "Fonds voor Wetenschappelijk Onderzoek Vlaanderen" for its financial support; Koen Delaere has a FWO-V scholarship. The authors thank the Belgian Ministry of Scientific Research for granting the IUAP No.P4/20 on Coupled Problems in Electromagnetic Systems. The research Council of the K.U.Leuven supports the basic numerical research.

Reference

[1] O.C. Zienkiewicz, R.L. Taylor, *The Finite Element Method*, McGraw-Hill 1989.

[2] P.P. Silvester, R.L. Ferrari, *Finite Elements for Electrical Engineers, Third Edition*, Cambridge University Press, 1996.

[3] J.L. Coulomb, G. Meunier, "Finite element implementation of virtual work principle for magnetic or electric force or torque computation", *IEEE Trans.Magn*. Vol.20 no 5, pp.1894-1896, 1984.

[4] Z. Ren, A. Razek, "Local force computation in deformable bodies using edge elements", *IEEE Trans.Magn.*, Vol.28, 1992, pp.1212-1215.

[5] J.T. Oden, *Mechanics of Elastic Structures*, McGraw-Hill 1967.

[6] W.T. Thomson, *Theory of Vibrations with Applications*, *Fourth Edition*, Prentice-Hall 1993.

[7] L. Meirovich, *Computational Methods in Structural Dynamics*, Sijthoff & Noordhoff 1980.

[8] W. Heylen, S. Lammens, P. Sas, *Modal Analysis Theory and Testing*, Katholieke Universiteit Leuven, Dept. Mechanics, Heverlee, Belgium, 1997.

[9] D. Verdyck, R. Belmans, "An acoustic model for a permanent magnet machine: Modal shapes and magnetic forces", *IEEE Trans. on industry applications (IAS)*, 1994, Vol.30 no.6, pp.1625-1631.